INTERNATIONAL CONFERENCE ON ELECTROMECHANICAL AND POWER SYSTEMS
October 4-6, 2007 - Chişinău, Rep.Moldova

MODELING AND OPTIMIZATION OF HIGH CURRENTS DISMOUNTABLE CONTACTS

Ioan POPA[1], Ioan CAUȚIL[1], Dan FLORICĂU[2], Florin OCOLEANU[1]

[1]University of Craiova, [2]Politehnica University of Bucharest, ipopa@elth.ucv.ro

Abstract **– The paper presents an electro-thermal numerical model which can be used for the modelling and optimization of dismountable contacts of high currents by neglecting the skin effect (by taking into account the very large ratio, near to 10, of the dimensions of cross-section of the current lead for which the skin effect is very weak). The numerical model is obtained by the coupling of the electrokinetic field problem with the thermal field problem. The coupling is carried out by the source term of the differential equation which describes the thermal field. The source term depends on the electric conductivity which varies according to the temperature. The model allows the calculation of the distribution in the space of the electric quantities (electric potential, the gradient of potential and the current density) and of the thermal quantities (the temperature, the temperature gradient, the Joule losses and heat flow). In the contact zone, it appears a heating larger than that of the current lead caused by the contact resistance. The additional heating, caused by the contact resistance, is simulated by an additional source injected on the surface of contact. The contact resistance can be calculated using different models. For an imposed limiting value of the temperature, using the model, one can determine the optimal geometry of dismountable contact.**

Keywords: *numerical modeling, dismountable contacts, coupled problems, finite volumes, optimization.*

1. INTRODUCTION

The optimization of the dismountable contacts (Figure 1) for high currents (1250 – 6000 A), used in the design of electrical equipment in metal envelope, is possible by solution of a coupled problem, electrical and thermal. The dismountable contact of a system of bus bars has a non-uniform distribution of current density (figure 2) on the cross-section of the current leads. The non-uniform distribution of the current density implies a non-uniform distribution of source term in the thermal conduction equation.

The distribution of the electric quantities can be obtained by solving of Laplace equation for electric potential. The solution of this equation depends on the temperature through electric conductivity. In its turn the electric conductivity influences the source term in the thermal conduction equation and thus the value and the distribution of the temperature of electrical contact.

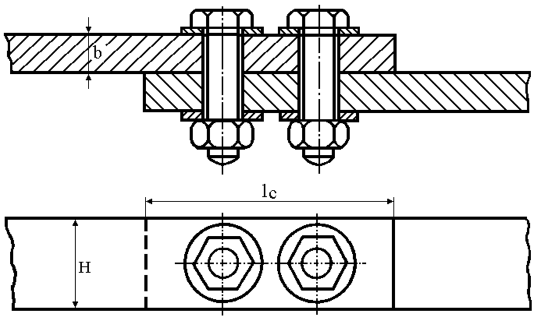

Figure 1: Typical dismountable contacts

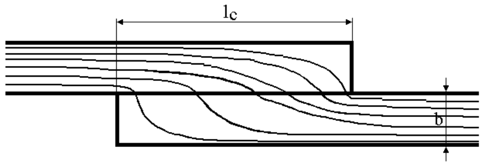

Figure 2: Current density distribution

Obtaining the correct distributions for the electric quantities (potential, intensity of the electric field, current density and losses by Joule effect) and thermic (the temperature, the gradient of temperature, density of the heat flow, the convection flow on the contact surface, etc) is possible by the coupling of the two problems, electric and thermal.

The numerical model allows the calculation of the constriction resistance (caused by the variation of the cross section of the current lead).

2. MATHEMATICAL MODEL

The mathematical model used for obtaining the numerical model has two components, the electrical model and the thermal model, coupled by the electric conductivity, which varies according to the temperature, $\sigma(T)$ and the source term $S(T) = \sigma(T)E^2 = \rho(T)J^2$.

2.1. Electrical Model

The electrical model is governed by a 2D model described by the Laplace equation for the electric potential:

$$\frac{\partial}{\partial x}\left(\sigma(T)\frac{\partial V}{\partial x}\right)+\frac{\partial}{\partial y}\left(\sigma(T)\frac{\partial V}{\partial y}\right)=0\,, \qquad (1)$$

where electric conductivity and thus the electrical resistance vary according to the temperature as:

$$\rho(T)=\rho_{20}\left(1+\alpha_R(T-20)\right) \qquad (2)$$

By knowing the electric potential, one can obtain the intensity of the electric field $\vec{E}=-\overrightarrow{grad}(V)$ and the current density $\vec{J}=\sigma\vec{E}$ (law of electric conduction).
The Joule losses (by the unit of volume) which represents the source term in the thermal conduction equation are calculated by the following relation:

$$S(T)=\vec{J}\cdot\vec{E}=\rho(T)J^2=\sigma(T)E^2 \qquad (3)$$

2.2. Thermal Model

The thermal model is governed by the thermal conduction equation in steady state:

$$\frac{\partial}{\partial x}\left(\lambda(T)\frac{\partial T}{\partial x}\right)+\frac{\partial}{\partial y}\left(\lambda(T)\frac{\partial T}{\partial y}\right)+S=0 \qquad (4)$$

where: λ - the thermal conductivity which is considered constant in the temperature range of the current lead (bellow $200\ ^{\circ}\mathrm{C}$).

3. DOMAIN OF ANALYSIS AND BOUNDARY CONDITIONS

One considers a simplified analysis domain which is presented in figures 3 and 4 where one neglects the existence of the fastening bolts.
The boundary conditions of the electrical model are presented in figure 3. In the general case, one knows the current I carrying the current lead and which determines a voltage drop V_1-V_2. In this model, one initializes a voltage drop for which one calculates the current which corresponds to it (at each iteration) and then in a iteration loop one modifies the voltage drop to obtain the desired value of the current.
The current which passes any section of the current lead is calculated by the following relation:

$$I=\int_S(\vec{J}\cdot\vec{n})dS \qquad (5)$$

where: $\vec{n}$ - the normal at S which is the cross-section of the current lead.
The two assembled bars are considered sufficiently long to set, on the boundaries AB and CD (figure 4) the boundary conditions of Neumann homogeneous type.
On the other borders, one sets boundary conditions of the convection type, with a global heat exchange coefficient h (by convection and radiation, $h=20$ W/m^{2}K) to the environment having the temperature T_∞ [3].

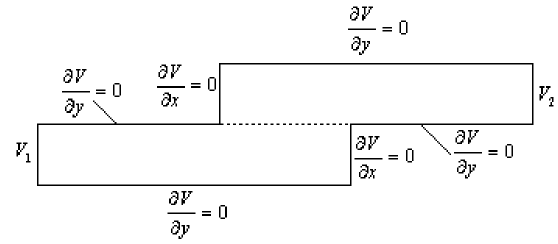

Figure 3: Analysis domain and boundary conditions for electrical model

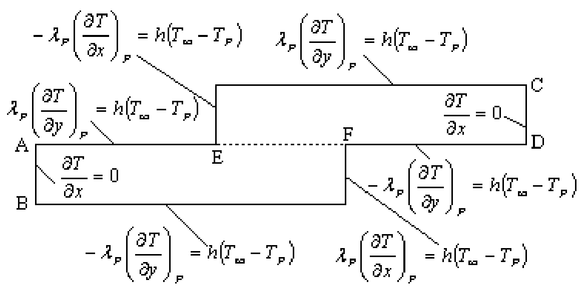

Figure 4: Analysis domain and boundary conditions for thermal model

4. NUMERICAL ALGORITHM

The numerical model is obtained by the discretization of the differential equations (1) and (4) by using the finite volumes method [1].
The coupled model is of alternate type [2] where the equations are solved separately and coupling is realized by the transfer of the data of one problem to the other. The two problems (electric and thermal) are integrated in the same source code and thus use the same mesh. The numerical algorithm is shown in figure 5.
The criterion of convergence of the coupled model was selected the value of the current, through the current lead, calculated using the relation (5). One used a mesh having 4293 nodes (with $\Delta x=\Delta y=0.002$ m).
The imposed error, for the electric model, was $\varepsilon_E=10^{-7}$ and for thermal model $\varepsilon_T=10^{-5}$. The error imposed for the coupled model was $\varepsilon_C=10^{-4}$.
The convergence of the coupled model is very fast, as we see in table 1 (for $l_c=100$ mm).
The numerical validation of the model was made using a simplified analysis domain, by using a current lead with variable cross-section [3].

The numerical validation of the results of this simplified model was made by using the software QuickField for the electrical model and the software Mirage (FEMM) for the thermal model. One can see a very good agreement between our results and the results obtained using the Mirage software.

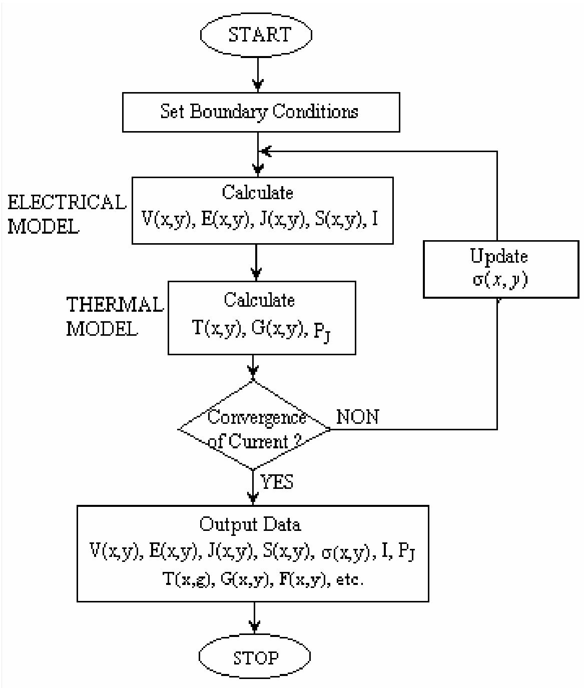

Figure 5: Simplified diagram of numerical algorithm

Iterations (coupled model)	Iterations (electrical model)	Iterations (thermal model)	Current [A]
1	388104	171986	1405.05
2	61053	45277	1262.67
3	26832	1	1264.66
4	1	1	1264.65

Table 1: Convergence of the iterative process for coupled model and current.

5. NUMERICAL RESULTS

The figures 6, 7, 8, 9 and 10 present some numerical results. The dimensions of the analysis domain are those of figure 6. The principal difficulty, in modelling and simulation the temperature distribution of a dismountable contact, is to take into account the resistance of contact (especially disturbance resistance because the resistance of constriction can be calculated by the model).

The optimization of the contact design supposes to determine the value of dimension l_c such that the maximum temperature, in the contact region, remains lower than the acceptable limiting value allowed by standards.

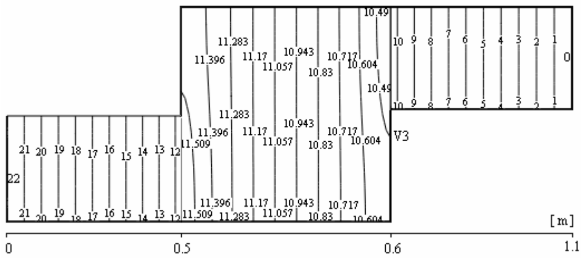

Figure 6: Potential distribution (in mV)

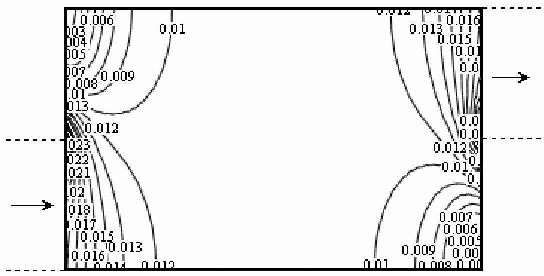

Figure 7: Electrical field distribution in the contact region (in V/m)

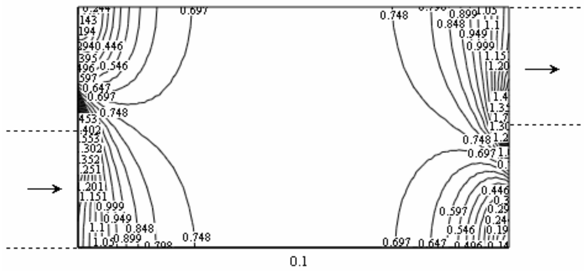

Figure 8: Current density distribution in the contact region (in A/mm^2)

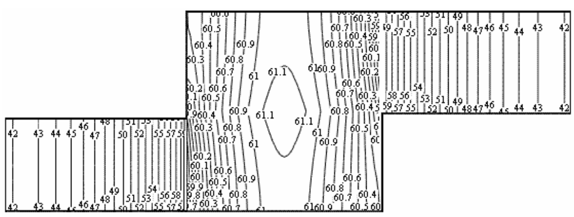

Figure 9: Temperature distribution (in ^oC)

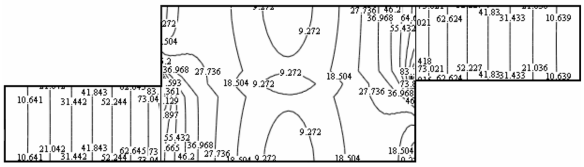

Figure 10: Temperature gradient distribution (in ^{o}C /m)

For the case presented in table 1 ($l_c = 100$ mm and $I = 1264.65$ A) the calculated losses by Joule effect are 28.89 W, while calculated ohmic losses are 24.91 W. The difference is due to the constriction resistance of the current lead.

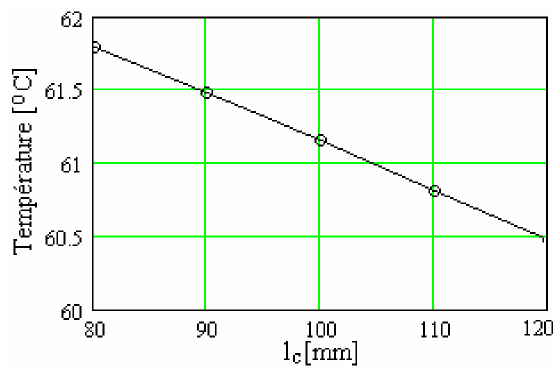

Figure 11: Maximum temperature of contact versus length of contact (for $S_c = 1.01\,\mathrm{kW}$).

6. CONTACT RESISTANCE MODEL

The source term determined by the contact resistance is calculated by the following relation:

$$S_c = \frac{R_c I^2}{(nc-1)\Delta x \Delta y\, H} \qquad (6)$$

where: Δx and Δy - the dimensions of the control volume, nc - the number of mesh points in the contact region (see fig. 17), H - the bus bar height (see fig. 12).

The contact resistance R_c is calculated with the following relation [5]:

$$R_c = \frac{\rho}{\pi a n} arctg \frac{\sqrt{d^2-a^2}}{a} - 1.2\frac{\rho\sqrt{d^2-a^2}}{A_a} + \frac{R_{ss}}{n\pi a^2} \qquad (7)$$

where: ρ - the electric resistivity, n - the number of contact points, $A_a = 8(2d)^2$ - the total area of contact (see fig. 18) and R_{ss} (in Ωm^2) - the specific resistance of oxide film of contact point.

The radius of contact surface a is calculated from Holm's relation:

$$a = \sqrt{\frac{F}{\pi n \xi H_d}} \qquad (8)$$

The relation (7) does not take into account the variation of contact resistance with temperature. To take it into account one can use the relation [5]:

$$R_c(T) = R_c(20)\left(1 + \frac{2}{3}\alpha_R (T-20)\right) \qquad (9)$$

where: α_R - the variation coefficient of electric resistivity with temperature.

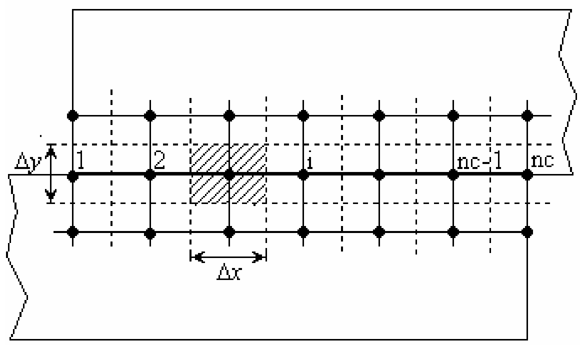

Figure 12: The mesh in contact region

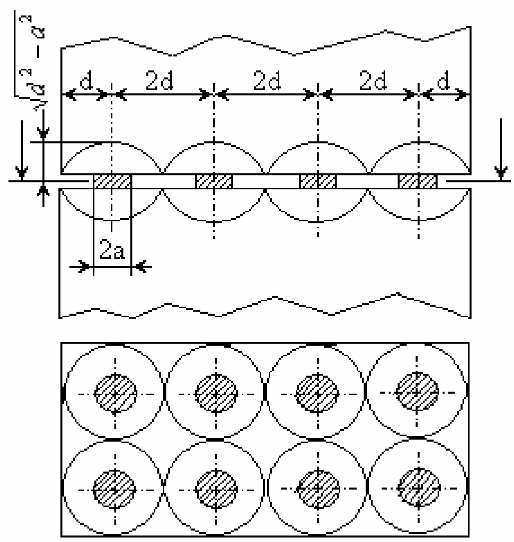

Figure 13: Physical model of contact region

The contact resistance model was implemented in numerical model of dismountable contact. For a constant value of the current ($I = 2275\,A$), varying the tightening force of the screws one can get the variation of the maximum temperature versus tightening force (see fig. 14)

A simplified model for electrical contact resistance between two bars was given by Greenwood. In the absence of oxide film of contact point the contact resistance a unit apparent contact aria is a function of surface asperities and bulk resistance [7]:

$$R_c = \left(\frac{\rho}{n}\right)\left(\frac{1}{2\bar{a}} + \frac{3\pi}{16\bar{l}}\right) \qquad (10)$$

where: ρ is the bulk resistivity of the contacting bodies, n is the number of contacting asperities per unit area, $\bar{a}$ is the average contacting radius of asperities and $\bar{l}$ is the average center-to-center distance between of contact asperities. The quantities $\bar{a}$ and $\bar{l}$ can be related to the yield strength (σ_{ys}), n and contact pressure (p). Finally the contact resistance can be expressed as an explicit function of apparent contact pressure p, bulk resistance ρ and the yield strength σ_{ys} of material. After further introducing the temperature dependency of σ_{ys} the contact resistance becomes an explicit function of temperature pressure and bulk resistivity for a given contact interface:

$$R_c = f(p, T, \rho) \qquad (11)$$

The summit of two surfaces in an electric joint that stay in metallic or quasimetallic contact form the so called a-spots [6]. The current lines bundle together to pass through the a-spots and cause the constriction resistance R_s. The number n, the shape and the area of a-apots are generally stochastic and depend on material parameters of the conductor material, on the topography of the joint surfaces and on the joint force. For simplicity it is often assumed that the a-spots are cicular. Looking at one single circular a-spot its constriction resistance R_{1s} depends on its radius a and on resistivity ρ of the conductor material. Under the assumption that the bulk material above and under the a-spot is infinite in volume the value of the constriction resistance can be calculated by means of Holm's ellipsoid model.

$$R_{1s} = \frac{\rho}{2a} \qquad (12)$$

If a single a-spot is completely covered with a thin film of the resistivity ρ_{ss} and the thickness s its film resistance R_{1ss} is given by

$$R_{1ss} = \frac{\rho_{ss} s}{\pi a^2} = \frac{\sigma_{ss}}{\pi a^2} \qquad (13)$$

with σ_{ss} as tunnel resistivity that is the resistance of the film across one cm^2.

The total resistance of an a-spot refered to as contact resistance results in the sum of the constriction resistance R_{1s} and the film resistance R_{1ss}.

The constriction resistance and the film resistance of electric joint for high current application are ruled by the electric flow through n parallel a-spots with a distance of s_{ij} from the i^{th} to the j^{th} a-spot.

In case that a large number of a-spots exists in close vicinity the electric flow through each a-spot depends on the electric flow through its neighbours. The constriction resistance of the joint is given by the resistance of the parallel connexion of n a-spots and an additional term that describes the interaction of the current flows [6]:

$$R_c = \frac{\rho}{2n\bar{a}} + \frac{\rho}{\pi n^2}\sum_{i=1}^{n}\sum_{j,j\neq i}^{n}\frac{1}{s_{ij}} \qquad (14)$$

where: $\bar{a}$ is the mean radius of all a-spots.

The number n and the mean radius $\bar{a}$ of the a-spots can then be determined from the topography of the joint surface and from the elastic and plastic deformation of the summits under the joint force.

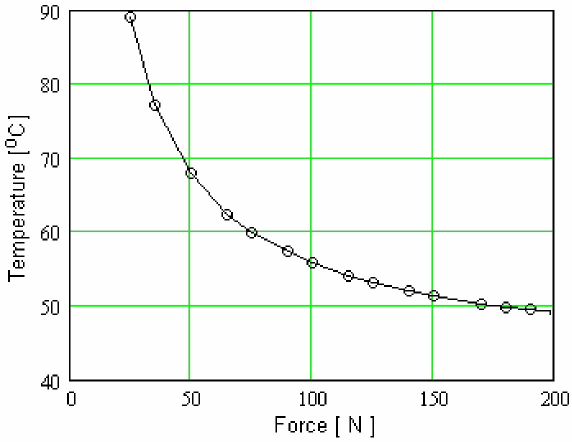

Figure 14: Maximum temperature in contact area versus tightening force (for $I = 2275\,A$)

The results presented in figure 14 are obtained with the model (7).

7. CONCLUSIONS

The elaborated model can be used for the optimization of the current leads of high currents with variable cross-section, such as the dismountable contacts. The model allows the calculation of the constriction resistance of current lead, the constriction resistance of contact region and takes into account the specific resistance of oxide film of contact point which is an important component of the contact resistance.

The results presented in figure 11 shows that it is possible to optimize the geometry and to reduce the mass of the contact. Numerical model elaborated

allows determination of the maximum temperature in the contact area as a function of the tightening force of the dismountable contact (see figure14). However an experimental validation of the numerical results is absolutely necessary.
An improvement of the model is possible taking into account the skin effect and the presence of the tightening screws.

References

[1] I. Popa, *Modélisation numérique du transfert thermique. Méthode des volumes finis*, Edition Universitaria, Craiova, 2002.

[2] G. Meunier, *Electromagnétisme et problèmes couplés,* Hermes Science, Paris, 2002.

[3] I. Popa, I. Cautil, D. Floricau, *Modèle numérique électrothermique pour l'optimisation des contacts démontables de forts courants,* Annals of the University of Craiova – Electrical Engineering Series, Year 30, Number 30, 2006, pp. 330 - 333.

[4] I. Popa, I. Cautil, D. Floricau, *Modeling and Optimization of High Currents Dismountable Contacts,* WSEAS Transaction on Power Systems, Issue 9, Volume 1, September 2006, pp. 1641 - 1646.

[5] G. Hortopan, *Electrical Swithcing Apparatus (in romanian),* Editura Tehnica, Bucharest, 1993.

[6] S. Schofy, J. Kindersberger, H Lobl, *Joint Resistance of Busbar-Joints with Randomly Rouggh Surfaces,* Procedings of 21th Conference on Electrical Contacts 2002, Zurich, pp. 230 - 237.

[7] Z. Feng, S.S. Babu, M.L. Santella, B.W. Riemer, J.E. Gould, *An Incrementally Coupled Electrical-Thermal-Mechanical Model for Resistance Spot Welding,* Procedings of 5th International Conference on Trends in Welding Research, Pine Mountain, GA, 1-5 June 1998, pp. 1 - 6.